



## Research Paper

# Endothelial NLRP3 inflammasome activation and arterial neointima formation associated with acid sphingomyelinase during hypercholesterolemia



Saisudha Koka<sup>a,b,\*</sup>, Min Xia<sup>a</sup>, Yang Chen<sup>a</sup>, Owais M. Bhat<sup>a</sup>, Xinxu Yuan<sup>a</sup>, Krishna M. Boini<sup>b</sup>, Pin-Lan Li<sup>a,\*\*</sup>

<sup>a</sup> Department of Pharmacology and Toxicology, Virginia Commonwealth University, Richmond, VA 23298, USA

<sup>b</sup> Department of Pharmacological and Pharmaceutical Sciences, College of Pharmacy, University of Houston, Houston, TX 77204, USA

## ARTICLE INFO

## Key words:

Inflammasome  
Ceramide  
Acid sphingomyelinase  
Atherosclerosis

## ABSTRACT

The NLRP3 inflammasome has been reported to be activated by atherogenic factors, whereby endothelial injury and consequent atherosclerotic lesions are triggered in the arterial wall. However, the mechanisms activating and regulating NLRP3 inflammasomes remain poorly understood. The present study tested whether acid sphingomyelinase (ASM) and ceramide associated membrane raft (MR) signaling platforms contribute to the activation of NLRP3 inflammasomes and atherosclerotic lesions during hypercholesterolemia. We found that 7-ketocholesterol (7-Keto) or cholesterol crystal (ChC) markedly increased the formation and activation of NLRP3 inflammasomes in mouse carotid arterial endothelial cells (CAECs), as shown by increased colocalization of NLRP3 with ASC or caspase-1, enhanced caspase-1 activity and elevated IL-1 $\beta$  levels, which were markedly attenuated by mouse *Asm* siRNA, ASM inhibitor- amitriptyline, and deletion of mouse *Asm* gene. In CAECs with NLRP3 inflammasome formation, membrane raft (MR) clustering with NADPH oxidase subunits was found remarkably increased as shown by CTXB (MR marker) and gp91<sup>phox</sup> aggregation indicating the formation of MR redox signaling platforms. This MR clustering was blocked by MR disruptor (MCD), ROS scavenger (Tempol) and TXNIP inhibitor (verapamil), accompanied by attenuation of 7-Keto or ChC-induced increase in caspase-1 activity. In animal experiments, Western diet fed mice with partially ligated left carotid artery (PLCA) were found to have significantly increased neointimal formation, which was associated with increased NLRP3 inflammasome formation and IL-1 $\beta$  production in the intima of *Asm*<sup>+/+</sup> mice but not in *Asm*<sup>-/-</sup> mice. These results suggest that *Asm* gene and ceramide associated MR clustering are essential to endothelial inflammasome activation and dysfunction in the carotid arteries, ultimately determining the extent of atherosclerotic lesions.

## 1. Introduction

The inflammasomes are an intracellular machinery responsible for the activation of inflammation in variety of tissues or organs [1]. Among different types of inflammasomes, the NLRP3 inflammasome has been well characterized, which consists of a proteolytic complex formed by Nlrp3, the adaptor protein ASC, and caspase-1. Caspase-1 is activated when the inflammasome complex is formed to produce active IL-1 $\beta$  and IL-18 by cleavage of their precursors. NLRP3 acts as the sensory component to recognize both endogenous and exogenous danger signals [2,3], when ASC and caspase-1 are recruited to form a protein complex, where caspase-1 is activated [3–7]. The active caspase-1 not only proteolytically cleaves IL-1 $\beta$  and/or IL-18 into their

biologically active form, but also produces other uncanonical effects such as release of damaging molecules like damage-associated molecular patterns (DAMPs), cell pyroptosis and alterations of cell membrane permeability, turning on the inflammatory response and directly inducing cell dysfunction or injury. There are increasing evidences that the activation of NLRP3 inflammasomes may not only contribute to autoinflammatory disorders, but also to a number of metabolic diseases including gout, silicosis, diabetes, liver toxicity, Alzheimer's disease and atherosclerosis [5,8–15]. In macrophages, NLRP3 inflammasome activation is critical for the foam cell formation and other atherosclerotic lesions upon proatherogenic stimuli such as cholesterol crystals (ChC) [13,16]. More interestingly, some non-atherogenic endanger factors also activate NLRP3 inflammasomes including adenosine triphosphate

\* Department of Pharmacological and Pharmaceutical Sciences, College of Pharmacy, University of Houston, 3455 Cullen Blvd, Room 463, Houston, TX 77204, USA.

\*\* Department of Pharmacology and Toxicology, Virginia Commonwealth University, School of Medicine, 1220 E Broad St, Room 3055, Richmond, VA 23298, USA.

E-mail addresses: [sskoka@uh.edu](mailto:sskoka@uh.edu) (S. Koka), [pin-lan.li@vcuhealth.org](mailto:pin-lan.li@vcuhealth.org) (P.-L. Li).

<http://dx.doi.org/10.1016/j.redox.2017.06.004>

Received 17 May 2017; Received in revised form 12 June 2017; Accepted 13 June 2017

Available online 15 June 2017

2213-2317/ © 2017 The Authors. Published by Elsevier B.V. This is an open access article under the CC BY-NC-ND license (<http://creativecommons.org/licenses/by-nc-nd/4.0/>).

(ATP), uric acid and DAMPs [4,11,15–22], which may enhance the susceptibility to atherosclerosis or other vascular diseases. However, it remains unclear how NLRP3 inflammasomes in endothelial cells (ECs) are activated by proatherogenic stimuli and how activated NLRP3 inflammasomes lead to endothelial injury and ultimate atherosclerotic lesions.

In this regard, it was shown in vascular ECs, membrane rafts (MRs) and their temporal-spatial organization within caveolae are reported to involve in signaling of vascular endothelial growth factors (VEGF) [23], nitric oxide synthase [24], H<sub>2</sub>O<sub>2</sub> [25], and prostanoid receptor activation [26]. Downstream effector response to MRs clustering in these ECs includes receptor autophosphorylation, cAMP production, caspase activation, decreases or increases in nitric oxide (NO), reorganization of the actin cytoskeleton and Ca<sup>2+</sup> mobilization [23,27–29]. Functionally, the MR-mediated signaling may contribute to the regulation of important endothelial functions such as endothelial barrier function [30], endothelium-dependent vasodilator or constrictor response [31–35], endothelial metabolic function [35,36], and its antithrombotic functions [37]. We have demonstrated that MRs clustering occurred in arterial ECs [35] upon stimulation of different agonists such as FasL, TNF- $\alpha$ , OxLDL, visfatin and endostatin induced aggregation of NADPH oxidase (NOX) subunits such as gp91<sup>phox</sup> and p47<sup>phox</sup> into MR clusters, whereby NOX activity markedly increased. This membrane MR-NOX cluster or complex that possesses redox signaling function has been referred to as an MR redox signaling platform [35,38,39]. ASM has been shown to importantly participate in the formation of this redox signaling platform in ECs [34,35,40] which is associated with lysosome trafficking and fusion to MR area via a SNARE-centered exocytic machinery [41,42]. However, the role of ASM-induced MR clustering in NLRP3 inflammasome activation remains unknown.

The present study hypothesized that ASM and its product of sphingomyeline, ceramide via the formation of MR redox signaling platforms mediate the activation of NLRP3 inflammasomes and thereby result in endothelial dysfunction and atherosclerosis. To test this hypothesis, we first determined whether the NLRP3 inflammasome is activated in response to cholesterol crystal (ChC) and 7-ketocholesterol (7-Keto) in ECs from *Asm* wild type and gene knockout mice. In the in vivo animal experiments, we examined whether endothelial NLRP3 inflammasome activation associated with enhanced ceramide production via ASM contributes to atherosclerotic lesions in the carotid arteries. Our results demonstrate that ASM and ceramide-associated MR clustering with NOX subunits in ECs is essential to endothelial inflammasome activation and dysfunction in the carotid arteries, which determines the extent of neointima formation in the carotid arteries during PLCA mouse model.

## 2. Material and methods

### 2.1. Cell culture and treatments

The mouse carotid arterial endothelial cells were isolated and characterized as described earlier [43]. For the proatherogenic stimulation, cells were treated with 7-Keto (10 ng/ml) or ChC (0.5 mg/ml) and then incubated for overnight. In case of inhibitors used, the cells were pretreated with amitriptyline (20  $\mu$ mol/L), methyl- $\beta$ -cyclodextrin (MCD, 1 mmol/L), Tempol (0.1 mmol/L) and verapamil (50  $\mu$ mol/L) for 30 min.

### 2.2. RNA interference of *Asm* gene

Small interference RNAs (siRNAs) were purchased from Santa Cruz. The sequence for *Asm* siRNA is: 5'-CACGTGGATGAGTTTGAGGT-3' which was confirmed to be effective in silencing *Asm* gene in different cells by the company. The scrambled small RNA (AATTCTCCGAACGTGTACGT) has been also confirmed as non-silencing double stranded RNA and was used as control in the present study.

Transfection of siRNA was performed using the siLentFect Lipid Reagent (Bio-Rad, CA, USA) according to the manufacturer's instructions.

### 2.3. Confocal microscopic analysis

For confocal analysis of inflammasome molecules, cultured CAECs were grown on glass coverslips, stimulated or unstimulated, fixed in 4% paraformaldehyde in phosphate-buffer saline (PFA/PBS) for 15 min. After being permeabilized with 0.1% Triton X-100/PBS and rinsed with PBS, the cells were incubated overnight at 4 °C with goat anti-NLRP3 (1:200, Abcam, MA) and rabbit anti-ASC (1:50, Enzo, PA) or rabbit anti-caspase-1 (1:100, Abcam, MA). To colocalize inflammasome molecules in the mouse carotid artery, double-immunofluorescent staining was performed using frozen tissue slides. After fixation, the slides were incubated overnight at 4 °C with goat anti-NLRP3 (1:200) and rabbit anti-ASC (1:50) or anti-caspase-1 (1:100). After washing, these slides probed with primary antibodies were incubated with Alexa-488- or Alexa-555-labeled secondary antibodies for 1 h at room temperature. The slides were mounted and subjected to examinations using a confocal laser scanning microscope (Fluoview FV1000, Olympus, Japan), with photos being taken and the colocalization of NLRP3 with ASC or caspase-1 analyzed by the Image Pro Plus 6.0 software (Media Cybernetics, Bethesda, MD, USA). The summarized colocalization efficiency data was expressed as Pearson correlation coefficient (PCC) as we described previously [44,45].

### 2.4. Immunofluorescent microscopic analysis of MR clusters

CAECs were grown on poly-L-lysine-coated glass coverslips. After fixation with 4% PFA, cells were incubated with Alexa Fluor 488 conjugated Cholera toxin B (Alexa488-CTXB, 2  $\mu$ g/ml, 2 h, Molecular Probes, CA), which binds with the MR-enriched ganglioside G<sub>M1</sub>. For dual-staining detection of the colocalization of MRs with gp91<sup>phox</sup>, the cells were first incubated with Alexa488-CTXB and then with anti-gp91<sup>phox</sup> (1: 200, BD Biosciences, CA), respectively, which was followed by corresponding Alexa555-conjugated secondary antibodies (1: 500, Invitrogen, NY). Then, the colocalization were visualized with confocal microscopy [43,46].

### 2.5. Caspase-1 activity and IL-1 $\beta$ production assay

After 7-Keto and ChC treatment with or without prior inhibitor, cells were harvested and homogenized to extract proteins for caspase-1 activity assay using a commercially available kit (Biovision, CA). The data was expressed as the fold change compared with control cells. In addition, the cell supernatant was also collected to measure the IL-1 $\beta$  production by a mouse IL-1 $\beta$  ELISA kit (Bender Medsystems, CA) according to the protocol described by the manufacturer.

### 2.6. FLICA staining

During the last hour of incubation, cells were labeled with FAM-YVAD-fmk caspase-1 FLICA™ kit (Immunochemistry, Bloomington, IN), which binds activated caspase-1. Flow cytometric analysis was performed according to manufacturer's manual. In brief, cells were washed two times with PBS and then incubated with 1  $\times$  FLICA for 1 h followed by two washes and analyzed with a Guava EasyCyte (Guava Technologies, Hayward, CA).

### 2.7. Endothelial permeability measurement

CAECs were cultured in 24-well transwell plates and treated as indicated for 12 h. The transwell inserts were moved into non-used wells with 200  $\mu$ l fresh media. 100  $\mu$ l Fluorescein isothiocyanate (FITC)-dextran (10 kDa, Invitrogen) solution was added into each

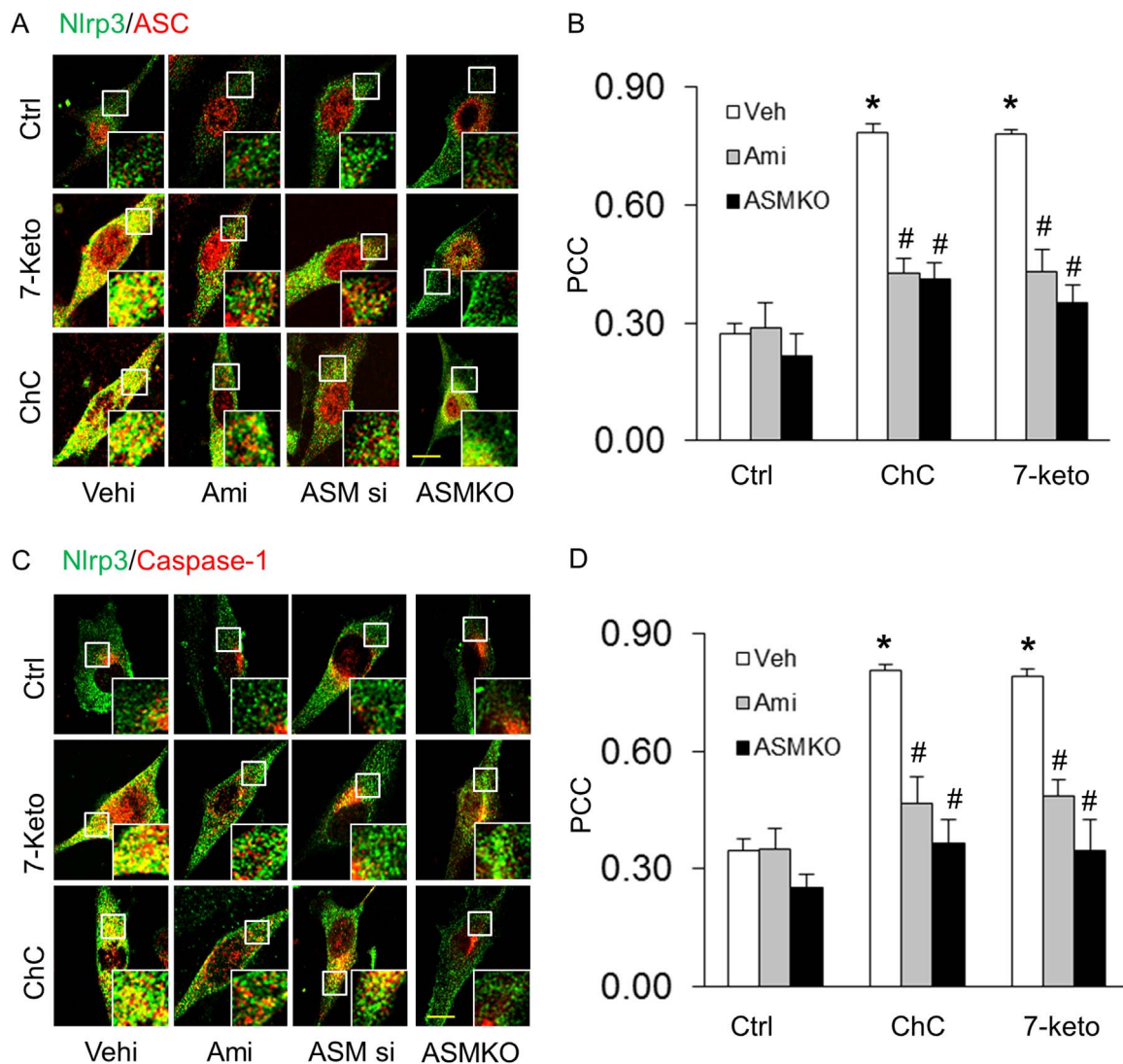


**Fig. 1.** *Asm* gene deletion abolished 7 Keto or ChC-induced NLRP3 inflammasome formation in CAECs. Representative fluorescent confocal microscopic images show the colocalization of NLRP3 with ASC (A) or NLRP3 with caspase-1 (C) in CAECs of *Asm*<sup>+/+</sup> and *Asm*<sup>-/-</sup> mice. \* Significant difference ( $P < 0.05$ ) compared to the values from control cells, #Significant difference ( $P < 0.05$ ) compared to the values from 7-Keto or ChC treated group. Scale bar: 5  $\mu$ m (A and C). Ami, Amitriptyline; *Asm* si, *Asm* siRNA: Cells were transfected with *Asm* siRNA and then stimulated with 7-Keto or ChC; Scr, scrambled: Cells were transfected with scramble RNA and then stimulated with 7-Keto or ChC.  $n = 6$  batches of cells.

insert and the plate was incubated at 37 °C for 2 h to allow fluorescein molecules flow through the endothelial cell monolayer. The inserts were then removed and fluorescent intensity in each well was determined at excitation/emission of 485/530 nm using a fluorescent microplate reader (FL  $\times$  800, BIO-TEK Instruments). The arbitrary fluorescence intensity was used to calculate the relative permeability [46].

## 2.8. Animals

*Asm*<sup>-/-</sup> mice (sphingomyelin phosphodiesterase 1 (*Smpd1*) is the gene symbol for ASM) and *Asm*<sup>+/+</sup> (male, 8 weeks of age, in house bred) were fed a normal diet (ND) or a Western diet (WD, Research Diets, NJ) for 4 weeks. All mice were genotyped by PCR and they are randomly distributed to different experimental groups. At the end point of experiments, blood samples were collected and these mice were sacrificed and carotid arteries were harvested for dual fluorescence staining and confocal analysis. All protocols were approved by the Institutional Animal Care and Use Committee of the Virginia Commonwealth University.

## 2.9. Partial ligation of left carotid artery

Eight weeks old male *Asm*<sup>+/+</sup> and *Asm*<sup>-/-</sup> mice were used [19]. All protocols were approved by the Institutional Animal Care and Use Committee of the Virginia Commonwealth University. Partial carotid ligation surgery was performed as previously reported by others [45,47,48]. In brief, animals were sedated with 2% isoflurane provided through a nose cone. Next, a ventral midline incision of 4–5 mm was made in the neck. Using blunt dissection, muscle layers were separated with curved forceps to expose the left carotid artery (LCA). Three (left external carotid, internal carotid, and occipital artery) out of four branches of the LCA were ligated using a 6-0 silk suture. The superior thyroid artery was left intact providing the sole source for blood circulation. The incision was then closed and the animals kept on a heating pad until they gained consciousness. After 14 days post-partial ligation, animals were sacrificed by cervical dislocation following the administration of anesthesia. Blood samples were collected; left and right carotid arteries were then harvested for immunohistochemistry, dual fluorescence staining and confocal analysis.

## 2.10. Immunohistochemistry

Formalin-fixed, paraffin-embedded carotid arterial tissue sections (4  $\mu$ m) were stained with primary antibodies (1:50 dilution) overnight at 4 °C after a 20 min wash with 3% H<sub>2</sub>O<sub>2</sub> and 30 min blocking with serum. The slides were sequentially treated with CHEMICON IHC Select HRP/DAB Kit (EMD Millipore, MA) according to the protocol described by the manufacturer. Finally, the slides were counterstained with hematoxylin. Negative controls were prepared by leaving out the primary antibodies.

## 2.11. Statistics

Data are presented as means  $\pm$  SE. Significant differences between and within multiple groups were examined using ANOVA for repeated measures, followed by Duncan's multiple-range test.  $P < 0.05$  was considered statistically significant.

## 3. Results

### 3.1. ASM activity inhibition or *Asm* gene knockout blocked the formation and activation of NLRP3 inflammasomes in carotid ECs

First, we tested whether ASM participates in 7-Keto or ChC-induced NLRP3 inflammasome formation and activation in CAECs of *Asm* mice. Using confocal microscopy, we demonstrated that 7-Keto (10 ng/ml) and ChC (0.5 mg/ml) increased colocalization of inflammasome molecules (NLRP3 with ASC or NLRP3 with caspase-1), as shown by yellow spots in carotid ECs from *Asm*<sup>+/+</sup> mice, which were blocked by ASM inhibitor, amitriptyline (Ami) or *Asm* siRNA transfection. However, in *Asm*<sup>-/-</sup> carotid ECs, these proatherogenic factors did not make NLRP3 inflammasome formation (Fig. 1A and C). The summarized data of quantitative co-localization of NLRP3 with ASC or with caspase-1 in CAECs were shown in Figs. 1B and D. Consistent with these findings, 7-Keto or ChC significantly increased the caspase-1 activity and IL- $\beta$  production in *Asm*<sup>+/+</sup> ECs (Fig. 2). Similar results were obtained when we quantified caspase-1 activation in CAECs using a cell-permeable fluorescent reagent, FLICA<sup>Casp1</sup>, which can specifically bind to the active form of caspase-1 (Fig. 2A and B). However, prior treatment with *Asm* gene silencing (*Asm* siRNA) or inhibitor (amitriptyline) almost completely blocked 7-Keto or ChC-induced increases in caspase-1 activity (Fig. 2A-C) and IL-1 $\beta$  production (Fig. 2D) in CAECs.

### 3.2. Involvement of MR redox signaling in 7-Keto and ChC-induced NLRP3 inflammasome activation

Earlier reports from our laboratory have demonstrated that NOX-mediated redox signaling contributes to Hcy-induced NLRP3 inflammasome activation in podocytes [42,60]. Therefore, we examined whether MR redox signaling pathway is involved in 7-Keto or ChC-induced NLRP3 inflammasomes activation in CAECs. In these experiments, CAECs were treated with 7-Keto or ChC and stained with Alexa Fluo 488-labeled cholera toxin B (CTXB, a MR marker) and anti-gp91<sup>phox</sup> antibody to colocalize MRs and gp91<sup>phox</sup>. As illustrated in Fig. 3A, both MRs and gp91<sup>phox</sup> were evenly distributed on the membrane of control cells. Upon 7-Keto or ChC stimulation, these MRs formed large and intense green fluorescent patches, which were colocalized with gp91<sup>phox</sup>. However, ASM inhibitor amitriptyline significantly attenuated the colocalization of gp91<sup>phox</sup> and MRs (Fig. 3B). Correspondingly, we found that prior treatment with MR blocker MCD, ROS scavenger, Tempol and TXNIP inhibitor verapamil significantly attenuated the 7-Keto or ChC-induced increases in caspase-1 activity (Fig. 3C).

### 3.3. ASM inhibition blocked 7-Keto or ChC-enhanced endothelial permeability in CAECs

Next, we determined the functional significance of NLRP3 inflammasome activation and examined its influence on 7-Keto or ChC-induced changes in barrier function of endothelial monolayers. As shown in Fig. 4, dextran flux significantly increased in CAECs treated with 7-Keto and ChC. This 7-Keto and ChC-induced hyperpermeability of CAECs was markedly reduced in the presence of *Asm* siRNA transfection or inhibitor of ASM.

#### 3.3.1. Endothelial inflammasome formation and activation in the carotid arteries of mice on the Western diet (WD)

As shown in Fig. 5A, confocal microscopy demonstrated that the colocalization of NLRP3 with ASC significantly increased as shown by yellow spots in the intima of the carotid arteries of WD-treated *Asm*<sup>+/+</sup> mice. This suggests the formation of NLRP3 inflammasomes in the endothelium of these arteries. In *Asm*<sup>-/-</sup> mice, however, such colocalization was much less detected. The summarized data of quantitative colocalization of NLRP3 with ASC in the carotid arteries were shown in Fig. 5B. In addition, the WD-induced IL-1 $\beta$  production in the intima was also abolished in *Asm*<sup>-/-</sup> mice (Fig. 5C).

#### 3.3.2. *Asm* deficiency prevented atherosclerotic lesions of the carotid arteries in 2 week partial ligation in mice

As described in our previous studies [45], a left carotid arterial partial ligation (PLCA) was surgically prepared after the experimental mice on the Western diet (WD) for two weeks. It was found that the Western diet markedly increased neointimal formation (as shown by open triangles in Fig. 6A) and the ratio of intimal vs. medium (shown by solid triangles) layers (I/M) in 2-week PLCA compared with those from *Asm*<sup>+/+</sup> mice. However, such WD-enhanced neointimal formation and increased I/M ratio in PLCA were markedly attenuated in *Asm*<sup>-/-</sup> mice. These results are summarized in Fig. 6B. It is clear that the I/M ratios in PLCA were not significantly different in ND-fed mice. However, the I/M ratios in PLCA dramatically increased in mice on the WD in *Asm*<sup>+/+</sup> mice, but not in *Asm*<sup>-/-</sup> mice. These results suggest that mouse *Asm* gene is essential to enhanced atherosclerotic lesions in the carotid arteries by the WD, which may be associated with the activation of NLRP3 inflammasomes.

### 3.4. Enhanced ASM and ceramide expression in the carotid arteries of *Asm*<sup>+/+</sup> mice fed the Western diet.

Furthermore, we investigated whether increased ASM expression and ceramide levels are correlated with the NLRP3 inflammasomes activation upon Western diet treatment. By immunohistochemistry and fluorescent confocal microscopy, we found that ASM expression and ceramide level in the endothelium of carotid arteries were increased in *Asm*<sup>+/+</sup> mice on the WD, but almost undetectable in *Asm*<sup>-/-</sup> mice (vWF as an endothelial marker to stain the intima) (Fig. 7). Taken together, these results suggest that ASM and its product ceramide may mediate the WD-induced NLRP3 inflammasome formation and activation in the carotid arteries of mice.

## 4. Discussion

The primary goal of the present study was to reveal whether ASM and ceramide associated MR redox signaling contributes to hypercholesterolemia-induced NLRP3 inflammasome formation, activation and consequent atherosclerosis. *In vitro* studies using primary cultures of CAECs and an *in vivo* animal model of hypercholesterolemia demonstrated that ASM and ceramide-associated MR clustering is necessary for the formation and activation of NLRP3 inflammasomes in ECs upon proatherogenic stimulation, thereby leading to endothelial dysfunction and ultimate atherosclerotic pathology. The findings for the first time

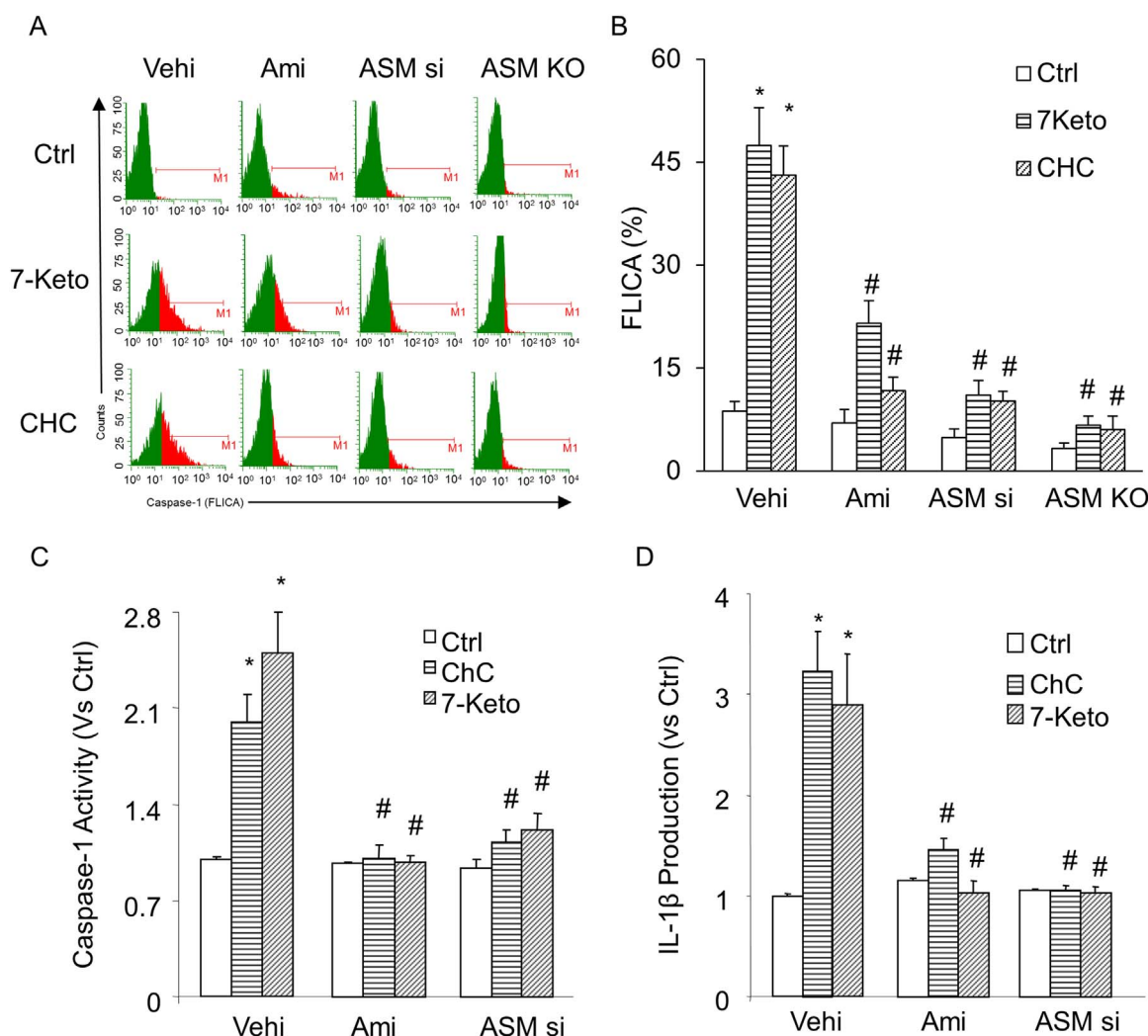


**Fig. 2.** Effects of the 7-Keto or ChC on caspase-1 activity and IL-1 $\beta$  production in CAECs. Caspase-1 activation was quantified using fluorescent FLICA<sup>Casp1</sup> reagent and analyzed by flow cytometry (A–B). Values are arithmetic means  $\pm$  SEM ( $n = 5$ – $6$  each group) of caspase-1 activity (C), IL-1 $\beta$  production (D) in CAECs of *Asm*<sup>+/+</sup> and *Asm*<sup>-/-</sup> mice with or without stimulation of 7-Keto or ChC and/or different inhibitors. \*Significant difference ( $P < 0.05$ ) compared to the values from control cells, #Significant difference ( $P < 0.05$ ) compared to the values from 7-Keto or ChC treated group. Vehi, Vehicle; Ami, Amitriptyline; Asm si and Asm siRNA: Cells were transfected with *Asm* siRNA and then stimulated with 7-Keto or ChC.

demonstrate the critical role of ASM and ceramide signaling pathway in the activation of NLRP3 inflammasomes and subsequent atherogenesis associated with hypercholesterolemia.

Although the NLRP3 inflammasome has been recently implicated in different auto-inflammatory diseases such as gout, myocardial infarction, and type II diabetes, obesity, glomerular injury and atherosclerosis [8,9,15,49–54], little is known how this inflammasome contributes to the initiation or development of atherosclerosis. In this regard, recent studies demonstrated that sphingolipid ceramide has been reported to initiate NLRP3 inflammasome formation and activation in different pathological conditions including insulin resistance, obesity, Alzheimer's disease, cystic fibrosis, glomerular injury and acute lung injury [44,53,55]. Ceramide released from the hydrolysis of membrane sphingomyelin by various sphingomyelinases such as ASM or neutral sphingomyelinase (NSM) or by *de novo* synthesis via serine palmitoyl-transferase (SPT) and ceramide synthase [56,57]. Ceramide is subsequently metabolized into sphingosine by ceramidases, and sphingosine can be further converted to S1P via sphingosine kinase in response to variety of stimuli including proinflammatory cytokines, oxidative stress, and increased levels of free fatty acids. It was reported that NLRP3 shRNA abolished the ceramide-induced inflammasome activation, production of proinflammatory cytokines and alveolar permeability in alveolar type II cells [55]. Furthermore, the acid

sphingomyelinase heterozygous mice have normalized pulmonary ceramide levels and prevented the NLRP3 inflammasome formation and activation in cystic fibrotic lungs [58]. However, it remains unknown whether ASM and ceramide signaling pathway mediates hypercholesterolemia-induced endothelial NLRP3 inflammasome activation and subsequent atherosclerosis. In the present study, we first confirmed that ChC or 7-Keto stimulation induced the formation and activation of the NLRP3 inflammasome complex in CAECs, as shown by colocalization of NLRP3 with ASC or NLRP3 with caspase-1 using confocal microscopy and by biochemical analysis of caspase-1 activity and production of IL-1 $\beta$ . However, such inflammasome formation and activation were abolished in CAECs from *Asm*<sup>+/+</sup> mice with prior treatment with *Asm* siRNA or ASM inhibitor, amitriptyline or *Asm* gene deletion (Figs. 1 and 2). In the *in vivo* studies, mice fed with the Western diet for 4 weeks has increased *Asm* gene expression and enhanced ceramide production in the carotid arteries in *Asm*<sup>+/+</sup> mice, but not in *Asm*<sup>-/-</sup> mice. Consistent with the increased ASM expression and enhanced ceramide production in the carotid arteries with partial ligation, the NLRP3 inflammasome formation (colocalization of NLRP3 with Asc) and activation (IL-1 $\beta$  production) were also largely increased. However, such effects were not seen in the carotid arteries of *Asm*<sup>-/-</sup> mice (Fig. 5). Taken together, these results clearly suggest that ASM mediates hypercholesterolemia-induced Nlrp3 inflammasome activation in ECs, which may contribute to

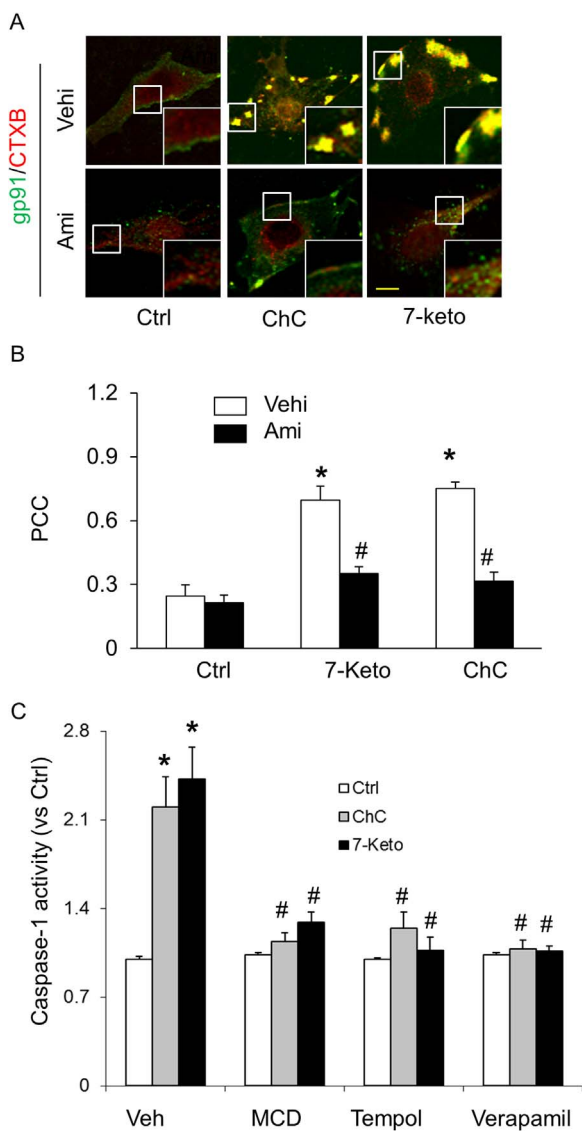


**Fig. 3.** Effects of MR-Redox signaling or TXNIP inhibition on 7-Keto or ChC-induced NLRP3 inflammasome activation in CAECs. A) Representative fluorescent confocal microscopic images of MR clusters and aggregation of gp91<sup>phox</sup> in CAECs. Alexa-488-CTXB for MR labeling was shown as a green color, and Texas Red conjugated anti gp91<sup>phox</sup> antibody was shown as red color. Yellow spots or patches in the overlaid images were defined as MR clusters with colocalization of gp91<sup>phox</sup>. Scale bar: 5 μm. B) Summarized data showing the effects of ASM inhibitor, amitriptyline on the formation of MR gp91<sup>phox</sup> clusters. Panel bars display means ± SEM of five experiments with analysis of more than 1000 CAECs. Ctrl: Control, Ami: Amitriptyline, ChC: cholesterol crystals, veh: vehicle. Values are arithmetic means ± SEM of caspase-1 activity (C) in CAECs with or without stimulation of 7-keto or ChC. MCD: Methyl-β-cyclodextrin. Tempo: 4-hydroxyl-tetramethylpiperidin-oxyl. \*P < 0.05 vs. Ctrl group; #P < 0.05 vs. 7-keto or ChC group (n = 5–6). (For interpretation of the references to color in this figure legend, the reader is referred to the web version of this article).

the development of neointima formation or atherogenic pathology. These results are in consistent with previous findings that high fat diet increased glomerular ceramide production due to the activation of ASM, where the increased ceramide production induced the formation and activation of NLRP3 inflammasome in glomeruli, contributing to the obesity-induced glomerular injury [59]. To our knowledge, the results from the present study provide the first experimental evidence showing the critical role of ASM in mediating endothelial inflammasome activation in response to proatherogenic stimulation.

The present study further examined the mechanism by which ChC or 7-Keto may induce NLRP3 inflammasomes activation in CAECs. It is well documented that several mechanisms underlying inflammasome

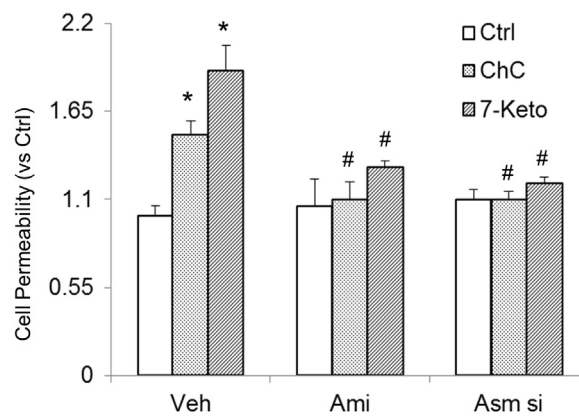


**Fig. 4.** Effects of ASM inhibition on 7-Keto or ChC-induced endothelial cell monolayer hyperpermeability in CAECs. Values are arithmetic means ± SEM (n = 6 each group) of cell permeability in CAECs of *Asm*<sup>+/+</sup> mice with or without stimulation of 7-Keto or ChC and/or different inhibitors. \*Significant difference (P < 0.05) compared to the values from control cells, #Significant difference (P < 0.05) compared to the values from 7-Keto or ChC treated group. Asm si: Asm siRNA; Ami: Amitriptyline (n = 5).

activation have been reported, including lysosome rupture, K<sup>+</sup> channel gating, and reactive oxygen species (ROS) activation [60,61]. Activation of the NLRP3 inflammasome by increased ROS is the most widely accepted and considered to be the most plausible mechanism, and this inflammasome is even considered as a general sensor for changes in cellular oxidative stress. In this regard, studies from our laboratory established that NOX-derived ROS activate NLRP3 inflammasomes in the pathogenesis of hHcy-induced glomerular sclerosis or adipokine visfatin-induced atherosclerosis [45,60]. This NOX activation in response to many different stimuli is due to the formation of MR redox signalosomes. These MR signalosomes use MR as a platform to conduct redox signaling, which are centered on the enzymatic NOX subunits clustering and activation to produce O<sub>2</sub><sup>•-</sup> [32,33]. NOX-derived ROS can act downstream to conduct transmembrane or intracellular signaling, leading to the redox regulation of cell and organ function [38]. We reported that different stimuli such as Hcy, visfatin, or ATP act on the cell membrane, stimulate ASM to produce and form ceramide-enriched MR platforms and thereby increase NOX-dependent O<sub>2</sub><sup>•-</sup> production from cells [32,46,60,62–65]. We have reported that these stimuli also activate the NLRP3 inflammasome, where this MR-redox signaling platform provide the O<sub>2</sub><sup>•-</sup> necessary to trigger NLRP3 inflammasome activation. Indeed, the present study found that ChC or 7-Keto stimulated the MR clustering and enhanced enrichment of NOX subunits in MR clusters. These results suggest that NOX subunits such as gp91<sup>phox</sup> were aggregated in response to ChC or 7-Keto stimulation. In addition, we also demonstrated that ChC or 7-Keto-induced caspase-1 activation was blocked by MR redox platform disruption, ROS scavenging, or gene silencing of TXNIP, a ROS-dependent binder of NLRP3 (Fig. 3C). Thus, our data suggest that MR redox signaling platforms are the major resources of ROS upon proatherogenic stimulations, which may be an important mechanism mediating ChC or 7-Keto-induced NLRP3 inflammasome activation in ECs.

To further address the functional significance of NLRP3 inflammasome activation in CAECs, we determined the role of ASM in mediating ChC or 7-Keto-induced enhancement of CAECs permeability. It is well known that the endothelial regulation of the passage of macromolecules and circulating cells from blood to tissues is a major target of oxidative stress and therefore endothelial dysfunction plays a critical role in the pathophysiology of many vascular and renal diseases [66,67]. In regard to the regulation of the vascular permeability, there is substantial evidence that oxidative stress increases the vascular endothelial permeability [68,69] and that increased endothelial permeability importantly contributes to the development of endothelial dysfunction. However, so far there is no direct evidence on the role of ASM in ChC or 7-Keto-

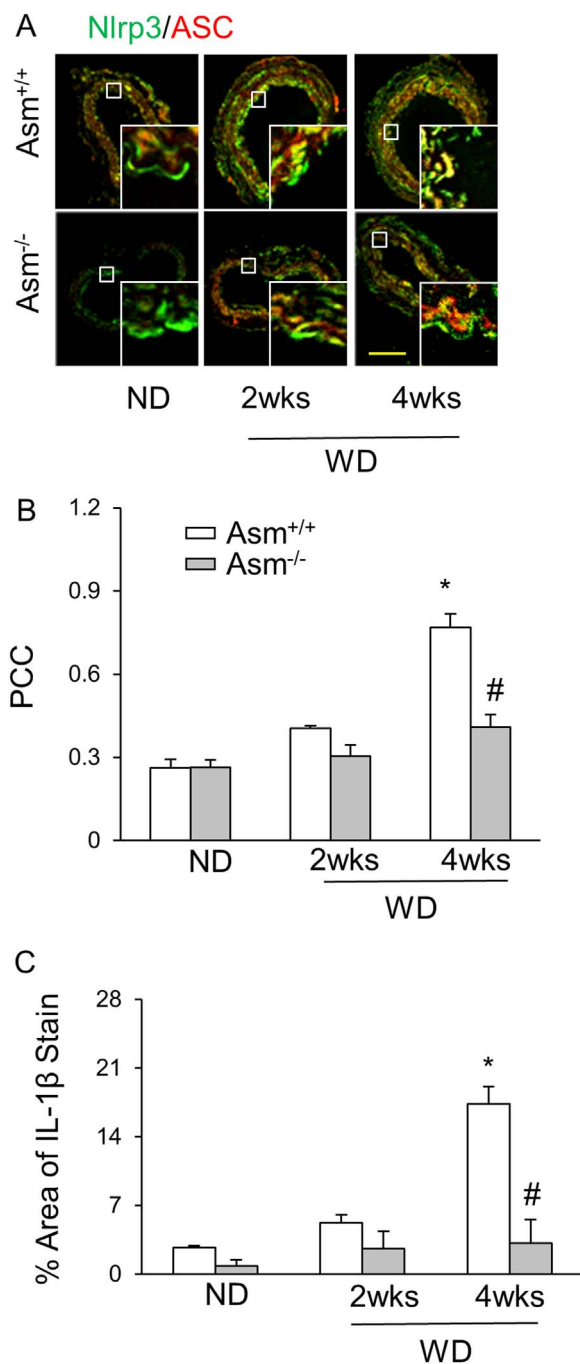


**Fig. 5.** NLRP3 inflammasome formation and activation in partially ligated carotid arteries of *Asm*<sup>+/+</sup> and *Asm*<sup>-/-</sup> mice fed with or without the WD. A: Colocalization of NLRP3 (green) with ASC (red), Scale bar: 50  $\mu$ m. B: summarized data of PCC of NLRP3 (green) with ASC (red). C: IL-1 $\beta$  production in the intima of control or Western diet-fed *Asm*<sup>+/+</sup> and *Asm*<sup>-/-</sup> mice. \* Significant difference ( $P < 0.05$ ) compared to the values from control mice fed on the normal diet; # Significant difference ( $P < 0.05$ ) compared to the values from mice on the Western diet. ND: Normal diet, WD: Western diet. (For interpretation of the references to color in this figure legend, the reader is referred to the web version of this article).

induced endothelial hyperpermeability. The present study has shown that ChC or 7-Keto increased the permeability of CAECs compared to control cells. This ChC or 7-Keto-induced increase in the CAECs permeability was markedly attenuated by pretreatment with ASM inhibitor amitriptyline or *Asm* gene silencing or deletion. Therefore, our data support the view that ASM-ROS-NLRP3 inflammasome axis is critically involved in hypercholesterolemia-induced endothelial barrier dysfunction. Corresponding to protection of ECs from ChC or 7-Keto-induced

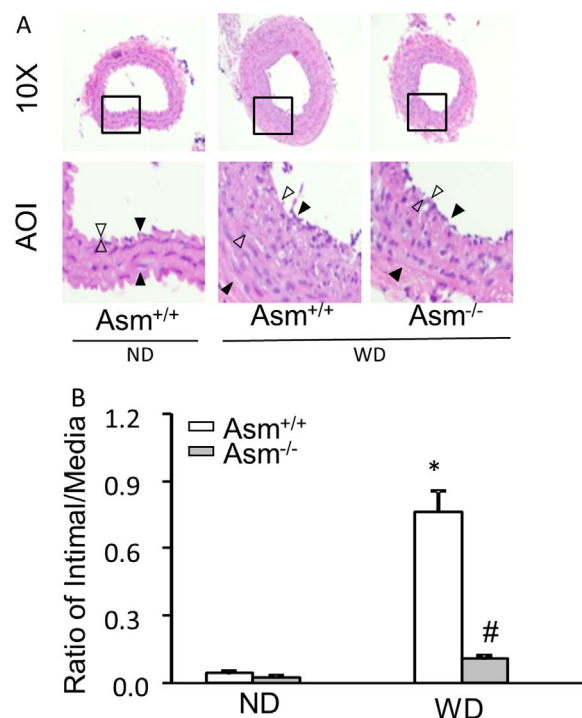


**Fig. 6.** Western diet enhanced the neointimal formation in PLCA. *Asm*<sup>+/+</sup> and *Asm*<sup>-/-</sup> mice were treated with the WD for 2 weeks and then used for PLCA. WD continued for another 2 weeks. (A) Photomicrographs of PLCA 2 weeks after the WD (H & E staining). AOI: Area of interest; black arrows denote the media area and white arrows indicate the intima area. (B) Quantitative analysis of vascular lesions in PLCA represented by the ratio of intima and media. \* $P < 0.05$  vs. vehicle control group; # $P < 0.05$  vs. WD group ( $n = 5-6$  mice per group).

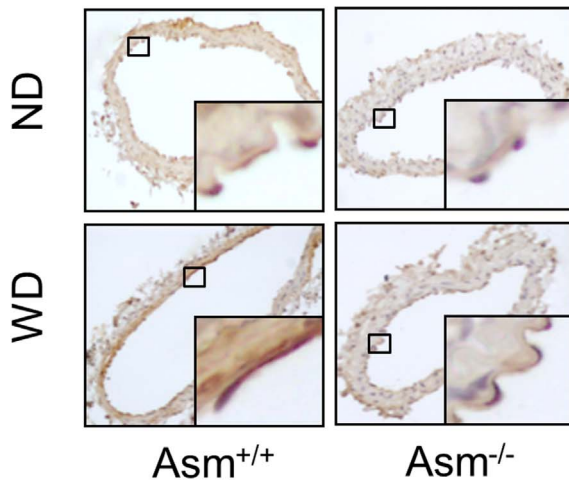
injury, inhibition of inflammasome activation by deletion of *Asm* gene significantly ameliorated hypercholesterolemia-induced atherosclerosis in mice, as shown by improved neointimal formation and ratio of intimal vs. medium layers (I/M) in 2-week partially ligated carotid arteries from mice on the Western diet. Inhibition of this inflammasome-triggering mechanism not only protects the endothelium of carotid arteries from injury, but also prevents atherosclerosis, which may be due to amelioration of both inflammatory response and uncanonical injurious effects induced by NLRP3 inflammasome activation. This ASM- and ceramide-associated MR clustering and related product such as  $O_2^{\cdot-}$  may act as redox-signaling messengers to activate the inflammasome, which serves as the bridging and amplifying mechanism leading to a robust inflammatory response that eventually progresses to atherosclerosis. These findings provide evidence that either targeting NLRP3 inflammasomes directly or targeting the mechanisms leading to their activation may be an effective therapeutic strategy for the prevention and early treatment of endothelial dysfunction and atherosclerosis.

In summary, the present study demonstrated that ASM and ceramide signaling plays a pivotal role in hypocholesterolemia-induced endothelial NLRP3 inflammasome formation and activation, which lead to endothelial dysfunction, vascular inflammation and cell phenotypic transition, and consequent atherosclerosis. Therefore, targeting ASM may be an important therapeutic strategy to prevent NLRP3 inflammasome activation and thereby protect the arteries from hypercholesterolemia-induced injury.

#### Conflicts of interests

The authors of this manuscript declare that they have no conflicts of interests.

## A Asm Expression



## B vWF/Ceramide

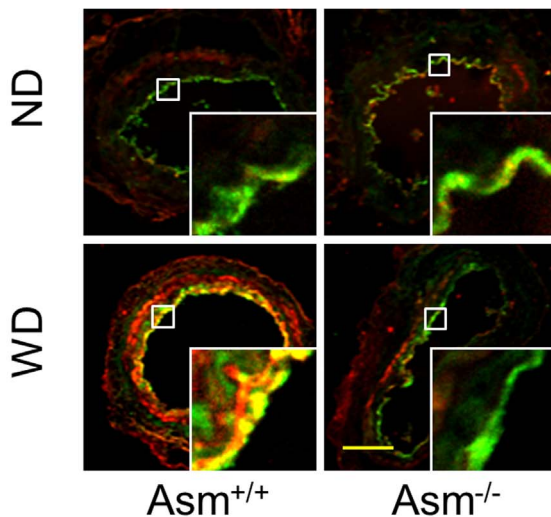


**Fig. 7.** Effects of the ND and WD on ASM expression and ceramide production in the carotid arteries of *Asm*<sup>+/+</sup> and *Asm*<sup>-/-</sup> mice. A: Representative immunohistochemical images show the ASM expression in the carotid arteries of mice fed with the ND or WD. B: Representative confocal microscopic images show the colocalization of vWF (an endothelial marker) vs. ceramide in the carotid arteries of mice fed with the ND or WD. Scale bar: 50  $\mu$ m.

### Acknowledgements

This work was supported by grants HL-57244, HL-075316, DK54927, HL-091464 (to P.L.) and DK104031 (to K.B.) from National Institutes of Health.

### References

- [1] A.A. Abdul-Sater, E. Koo, G. Hacker, D.M. Ojcius, Inflammasome-dependent caspase-1 activation in cervical epithelial cells stimulates growth of the intracellular pathogen *Chlamydia trachomatis*, *J. Biol. Chem.* 284 (39) (2009) 26789–26796.
- [2] C.A. Dinarello, M.Y. Donath, T. Mandrup-Poulsen, Role of IL-1 $\beta$  in type 2 diabetes, *Curr. Opin. Endocrinol. Diabetes Obes.* 17 (4) (2010) 314–321.
- [3] B. Samal, Y. Sun, G. Stearns, C. Xie, S. Suggs, I. McNiece, Cloning and characterization of the cDNA encoding a novel human pre-B-cell colony-enhancing factor, *Mol. Cell Biol.* 14 (2) (1994) 1431–1437.
- [4] M.P. Chen, F.M. Chung, D.M. Chang, J.C. Tsai, H.F. Huang, S.J. Shin, Y.J. Lee, Elevated plasma level of visfatin/pre-B cell colony-enhancing factor in patients with type 2 diabetes mellitus, *J. Clin. Endocrinol. Metab.* 91 (1) (2006) 295–299.
- [5] S. Freigang, F. Ampenberger, G. Spohn, S. Heer, A.T. Shamsheev, J. Kisielov, M. Hersberger, M. Yamamoto, M.F. Bachmann, M. Kopf, Nrf2 is essential for cholesterol crystal-induced inflammasome activation and exacerbation of atherosclerosis, *Eur. J. Immunol.* 41 (7) (2011) 2040–2051.
- [6] H. Poeck, M. Bscheider, O. Gross, K. Finger, S. Roth, M. Rebsamen, N. Hanneschlagler, M. Schlee, S. Rothenfusser, W. Barchet, et al., Recognition of RNA virus by RIG-I results in activation of CARD9 and inflammasome signaling for interleukin 1 beta production, *Nat. Immunol.* 11 (1) (2010) 63–69.
- [7] S.M. Srinivasula, J.L. Poyet, M. Razmara, P. Datta, Z. Zhang, E.S. Alnemri, The PYRIN-CARD protein ASC is an activating adaptor for caspase-1, *J. Biol. Chem.* 277 (24) (2002) 21119–21122.
- [8] C. Dostert, V. Petrilli, R. Van Bruggen, C. Steele, B.T. Mossman, J. Tschopp, Innate immune activation through Nalp3 inflammasome sensing of asbestos and silica, *Science* 320 (5876) (2008) 674–677.
- [9] A.B. Imaeda, A. Watanabe, M.A. Sohail, S. Mahmood, M. Mohamadnejad, F.S. Sutterwala, R.A. Flavell, W.Z. Mehal, Acetaminophen-induced hepatotoxicity in mice is dependent on Tlr9 and the Nalp3 inflammasome, *J. Clin. Investig.* 119 (2) (2009) 305–314.
- [10] T.L. Lewis, D. Cao, H. Lu, R.A. Mans, Y.R. Su, L. Jungbauer, M.F. Linton, S. Fazio, M.J. LaDu, L. Li, Overexpression of human apolipoprotein A-I preserves cognitive function and attenuates neuroinflammation and cerebral amyloid angiopathy in a mouse model of Alzheimer disease, *J. Biol. Chem.* 285 (47) (2010) 36958–36968.
- [11] F. Martinon, V. Petrilli, A. Mayor, A. Tardivel, J. Tschopp, Gout-associated uric acid crystals activate the NALP3 inflammasome, *Nature* 440 (7081) (2006) 237–241.
- [12] P. Menu, M. Pellegrin, J.F. Aubert, K. Bouzourene, A. Tardivel, L. Mazzolai, J. Tschopp, Atherosclerosis in ApoE-deficient mice progresses independently of the NLRP3 inflammasome, *Cell Death Dis.* 2 (2011) e137.
- [13] K. Rajamaki, J. Lappalainen, K. Oorni, E. Valimaki, S. Matikainen, P.T. Kovanen, K.K. Eklund, Cholesterol crystals activate the NLRP3 inflammasome in human macrophages: a novel link between cholesterol metabolism and inflammation, *PLoS One* 5 (7) (2010) e11765.
- [14] A. Salminen, J. Ojala, T. Suuronen, K. Kaamiranta, A. Kauppinen, Amyloid-beta oligomers set fire to inflammasomes and induce Alzheimer's pathology, *J. Cell Mol. Med.* 12 (6A) (2008) 2255–2262.
- [15] R. Zhou, A. Tardivel, B. Thorens, I. Choi, J. Tschopp, Thioredoxin-interacting protein links oxidative stress to inflammasome activation, *Nat. Immunol.* 11 (2) (2010) 136–140.
- [16] P. Duewell, H. Kono, K.J. Rayner, C.M. Sirois, G. Vladimer, F.G. Bauernfeind, G.S. Abela, L. Franchi, G. Nunez, M. Schnurr, et al., NLRP3 inflammasomes are required for atherosclerosis and activated by cholesterol crystals, *Nature* 464 (7293) (2010) 1357–1361.
- [17] N. Busso, A. So, Mechanisms of inflammation in gout, *Arthritis Res. Ther.* 12 (2) (2010) 206.
- [18] A. Halle, V. Hornung, G.C. Petzold, C.R. Stewart, B.G. Monks, T. Reinheckel, K.A. Fitzgerald, E. Latz, K.J. Moore, D.T. Golenbock, The NALP3 inflammasome is involved in the innate immune response to amyloid-beta, *Nat. Immunol.* 9 (8) (2008) 857–865.
- [19] S. Mariathasan, K. Newton, D.M. Monack, D. Vucic, D.M. French, W.P. Lee, M. Roose-Girma, S. Erickson, V.M. Dixit, Differential activation of the inflammasome by caspase-1 adaptors ASC and Ipaf, *Nature* 430 (6996) (2004) 213–218.
- [20] F. Martinon, K. Burns, J. Tschopp, The inflammasome: a molecular platform triggering activation of inflammatory caspases and processing of proIL-1 $\beta$ , *Mol. Cell* 10 (2) (2002) 417–426.
- [21] R. Stienstra, C.J. Tack, T.D. Kanneganti, L.A. Joosten, M.G. Netea, The inflammasome puts obesity in the danger zone, *Cell Metab.* 15 (1) (2012) 10–18.
- [22] T. Strowig, J. Henao-Mejia, E. Elinav, R. Flavell, Inflammasomes in health and disease, *Nature* 481 (7381) (2012) 278–286.
- [23] S. Ikeda, M. Ushio-Fukai, L. Zuo, T. Tojo, S. Dikalov, N.A. Patrushev, R.W. Alexander, Novel role of ARF6 in vascular endothelial growth factor-induced signaling and angiogenesis, *Circ. Res.* 96 (4) (2005) 467–475.
- [24] K.A. Pritchard, A.W. Ackerman, J. Ou, M. Curtis, D.M. Smalley, J.T. Fontana, M.B. Stemmer, W.C. Sessa, Native low-density lipoprotein induces endothelial nitric oxide synthase dysfunction: role of heat shock protein 90 and caveolin-1, *Free Radic. Biol. Med.* 33 (1) (2002) 52–62.
- [25] B. Yang, V. Rizzo, TNF-alpha potentiates protein-tyrosine nitration through activation of NADPH oxidase and eNOS localized in membrane rafts and caveolae of bovine aortic endothelial cells, *Am. J. Physiol. Heart Circ. Physiol.* 292 (2) (2007) H954–H962.
- [26] R.S. Ostrom, R.A. Bunday, P.A. Insel, Nitric oxide inhibition of adenylyl cyclase type 6 activity is dependent upon lipid rafts and caveolin signaling complexes, *J. Biol. Chem.* 279 (19) (2004) 19846–19853.
- [27] K. Hossain, A.A. Akhand, Y. Kawamoto, J. Du, K. Takeda, J. Wu, M. Yoshihara, H. Tsuboi, M. Kato, H. Suzuki, et al., Caspase activation is accelerated by the inhibition of arsenite-induced, membrane rafts-dependent Akt activation, *Free Radic. Biol. Med.* 34 (5) (2003) 598–606.
- [28] Y.C. Li, M.J. Park, S.K. Ye, C.W. Kim, Y.N. Kim, Elevated levels of cholesterol-rich lipid rafts in cancer cells are correlated with apoptosis sensitivity induced by cholesterol-depleting agents, *Am. J. Pathol.* 168 (4) (2006) 1107–1118 (quiz1404–1105).
- [29] S.A. Wickstrom, K. Alitalo, J. Keski-Oja, Endostatin associates with lipid rafts and induces reorganization of the actin cytoskeleton via down-regulation of RhoA activity, *J. Biol. Chem.* 278 (39) (2003) 37895–37901.
- [30] F.A. Sanchez, N.B. Savalia, R.G. Duran, B.K. Lal, M.P. Boric, W.N. Duran, Functional significance of differential eNOS translocation, *Am. J. Physiol. Heart Circ. Physiol.* 291 (3) (2006) H1058–H1064.
- [31] J.X. Bao, S. Jin, F. Zhang, Z.C. Wang, N. Li, P.L. Li, Activation of membrane NADPH oxidase associated with lysosome-targeted act phagomyelinase in coronary endothelial cells, *Antioxid. Redox Signal.* 12 (6) (2010) 703–712.

- [32] S. Jin, F. Yi, P.L. Li, Contribution of lysosomal vesicles to the formation of lipid raft redox signaling platforms in endothelial cells, *Antioxid. Redox Signal.* 9 (9) (2007) 1417–1426.
- [33] S. Jin, Y. Zhang, F. Yi, P.L. Li, Critical role of lipid raft redox signaling platforms in endostatin-induced coronary endothelial dysfunction, *Arterioscler. Thromb. Vasc. Biol.* 28 (3) (2008) 485–490.
- [34] A.Y. Zhang, E.G. Teggatz, A.P. Zou, W.B. Campbell, P.L. Li, Endostatin uncouples NO and Ca<sup>2+</sup> response to bradykinin through enhanced O<sub>2</sub><sup>•-</sup> production in the intact coronary endothelium, *Am. J. Physiol. Heart Circ. Physiol.* 288 (2) (2005) H686–H694.
- [35] A.Y. Zhang, F. Yi, G. Zhang, E. Gulbins, P.L. Li, Lipid raft clustering and redox signaling platform formation in coronary arterial endothelial cells, *Hypertension* 47 (1) (2006) 74–80.
- [36] S. Patschan, J. Chen, A. Polotskaia, N. Mendelev, J. Cheng, D. Patschan, M.S. Goligorsky, Lipid mediators of autophagy in stress-induced premature senescence of endothelial cells, *Am. J. Physiol. Heart Circ. Physiol.* 294 (3) (2008) H1119–H1129.
- [37] J.A. Lopez, I. del Conde, C.N. Shrimpton, Receptors, rafts, and microvesicles in thrombosis and inflammation, *J. Thromb. Haemost.* 3 (8) (2005) 1737–1744.
- [38] P.L. Li, Y. Zhang, F. Yi, Lipid raft redox signaling platforms in endothelial dysfunction, *Antioxid. Redox Signal.* 9 (9) (2007) 1457–1470.
- [39] Y.M. Wei, X. Li, J. Xiong, J.M. Abais, M. Xia, K.M. Boini, Y. Zhang, P.L. Li, Attenuation by statins of membrane raft-redox signaling in coronary arterial endothelium, *J. Pharmacol. Exp. Ther.* 345 (2) (2013) 170–179.
- [40] J.X. Bao, M. Xia, J.L. Poklis, W.Q. Han, C. Brimson, P.L. Li, Triggering role of acid sphingomyelinase in endothelial lysosome-membrane fusion and dysfunction in coronary arteries, *Am. J. Physiol. Heart Circ. Physiol.* 298 (3) (2010) H992–H1002.
- [41] W.Q. Han, M. Xia, M. Xu, K.M. Boini, J.K. Ritter, N.J. Li, P.L. Li, Lysosome fusion to the cell membrane is mediated by the dysferlin C2A domain in coronary arterial endothelial cells, *J. Cell Sci.* 125 (Pt 5) (2012) 1225–1234.
- [42] W.Q. Han, M. Xia, C. Zhang, F. Zhang, M. Xu, N.J. Li, P.L. Li, SNARE-mediated rapid lysosome fusion in membrane raft clustering and dysfunction of bovine coronary arterial endothelium, *Am. J. Physiol. Heart Circ. Physiol.* 301 (5) (2011) H2028–H2037.
- [43] X. Li, W.Q. Han, K.M. Boini, M. Xia, Y. Zhang, P.L. Li, TRAIL death receptor 4 signaling via lysosome fusion and membrane raft clustering in coronary arterial endothelial cells: evidence from ASM knockout mice, *J. Mol. Med.* 91 (1) (2013) 25–36.
- [44] K.M. Boini, M. Xia, J.M. Abais, G. Li, A.L. Pitzer, T.W. Gehr, Y. Zhang, P.L. Li, Activation of inflammasomes in podocyte injury of mice on the high fat diet: effects of ASC gene deletion and silencing, *Biochim Biophys. Acta* 1843 (5) (2014) 836–845.
- [45] M. Xia, K.M. Boini, J.M. Abais, M. Xu, Y. Zhang, P.L. Li, Endothelial NLRP3 inflammasome activation and enhanced neointima formation in mice by adipokine visfatin, *Am. J. Pathol.* 184 (5) (2014) 1617–1628.
- [46] K.M. Boini, C. Zhang, M. Xia, W.Q. Han, C. Brimson, J.L. Poklis, P.L. Li, Visfatin-induced lipid raft redox signaling platforms and dysfunction in glomerular endothelial cells, *Biochim. Biophys. Acta* 1801 (12) (2010) 1294–1304.
- [47] D. Nam, C.W. Ni, A. Rezvan, J. Suo, K. Budzyn, A. Llanos, D. Harrison, D. Giddens, H. Jo, Partial carotid ligation is a model of acutely induced disturbed flow, leading to rapid endothelial dysfunction and atherosclerosis, *Am. J. Physiol. Heart Circ. Physiol.* 297 (4) (2009) H1535–H1543.
- [48] H. Merino, S. Parthasarathy, D.K. Singla, Partial ligation-induced carotid artery occlusion induces leukocyte recruitment and lipid accumulation—a shear stress model of atherosclerosis, *Mol. Cell Biochem.* 372 (1–2) (2013) 267–273.
- [49] B.H. Lee, D.M. Hwang, N. Palaniyar, S. Grinstein, D.J. Philpott, J. Hu, Activation of P2X(7) receptor by ATP plays an important role in regulating inflammatory responses during acute viral infection, *PLoS One* 7 (4) (2012) e35812.
- [50] I. Bjarnason, C. O'Morain, A.J. Levi, T.J. Peters, Absorption of 51chromium-labeled ethylenediaminetetraacetate in inflammatory bowel disease, *Gastroenterology* 85 (2) (1983) 318–322.
- [51] T. Hornig, G.S. Hotamisligil, Linking the inflammasome to obesity-related disease, *Nat. Med.* 17 (2) (2011) 164–165.
- [52] R. Stienstra, L.A. Joosten, T. Koenen, B. van Tits, J.A. van Diepen, S.A. van den Berg, P.C. Rensen, P.J. Voshol, G. Fantuzzi, A. Hijmans, et al., The inflammasome-mediated caspase-1 activation controls adipocyte differentiation and insulin sensitivity, *Cell Metab.* 12 (6) (2010) 593–605.
- [53] B. Vandanmagsar, Y.H. Youm, A. Ravussin, J.E. Galgani, K. Stadler, R.L. Mynatt, E. Ravussin, J.M. Stephens, V.D. Dixit, The NLRP3 inflammasome instigates obesity-induced inflammation and insulin resistance, *Nat. Med.* 17 (2) (2011) 179–188.
- [54] D. De Nardo, E. Latz, NLRP3 inflammasomes link inflammation and metabolic disease, *Trends Immunol.* 32 (8) (2011) 373–379.
- [55] N. Kolliputi, L. Galam, P.T. Parthasarathy, S.M. Tipparaju, R.F. Lockey, NALP-3 inflammasome silencing attenuates ceramide-induced transepithelial permeability, *J. Cell Physiol.* 227 (9) (2012) 3310–3316.
- [56] K.M. Boini, M. Xia, C. Li, C. Zhang, L.P. Payne, J.M. Abais, J.L. Poklis, P.B. Hylemon, P.L. Li, Acid sphingomyelinase gene deficiency ameliorates the hyperhomocysteinemia-induced glomerular injury in mice, *Am. J. Pathol.* 179 (5) (2011) 2210–2219.
- [57] K.M. Boini, C. Zhang, M. Xia, J.L. Poklis, P.L. Li, Role of sphingolipid mediator ceramide in obesity and renal injury in mice fed a high-fat diet, *J. Pharmacol. Exp. Ther.* 334 (3) (2010) 839–846.
- [58] H. Grassme, A. Carpinteiro, M.J. Edwards, E. Gulbins, K.A. Becker, Regulation of the inflammasome by ceramide in cystic fibrosis lungs, *Cell Physiol. Biochem.* 34 (1) (2014) 45–55.
- [59] K.M. Boini, M. Xia, S. Koka, T.W. Gehr, P.L. Li, Instigation of NLRP3 inflammasome activation and glomerular injury in mice on the high fat diet: role of acid sphingomyelinase gene, *Oncotarget* 7 (14) (2016) 19031–19044.
- [60] J.M. Abais, C. Zhang, M. Xia, Q. Liu, T. Gehr, K.M. Boini, P.L. Li, NADPH oxidase-mediated triggering of inflammasome activation in mouse podocytes and glomeruli during hyperhomocysteinemia, *Antioxid. Redox Signal.* (2012).
- [61] J.M. Abais, M. Xia, Y. Zhang, K.M. Boini, P.L. Li, Redox regulation of NLRP3 inflammasomes: ROS as trigger or effector? *Antioxid. Redox Signal.* 22 (13) (2015) 1111–1129.
- [62] X. Li, E. Gulbins, Y. Zhang, Role of kinase suppressor of ras-1 in lipopolysaccharide-induced acute lung injury, *Cell Physiol. Biochem.* 30 (4) (2012) 905–914.
- [63] M. Xia, C. Zhang, K.M. Boini, A.M. Thacker, P.L. Li, Membrane raft-lysosome redox signalling platforms in coronary endothelial dysfunction induced by adipokine visfatin, *Cardiovasc. Res.* 89 (2) (2011) 401–409.
- [64] F. Yi, S. Jin, F. Zhang, M. Xia, J.X. Bao, J. Hu, J.L. Poklis, P.L. Li, Formation of lipid raft redox signalling platforms in glomerular endothelial cells: an early event of homocysteine-induced glomerular injury, *J. Cell Mol. Med.* 13 (9B) (2009) 3303–3314.
- [65] C. Zhang, K.M. Boini, M. Xia, J.M. Abais, X. Li, Q. Liu, P.L. Li, Activation of Nod-like receptor protein 3 inflammasomes turns on podocyte injury and glomerular sclerosis in hyperhomocysteinemia, *Hypertension* 60 (1) (2012) 154–162.
- [66] H. Lum, K.A. Roebuck, Oxidant stress and endothelial cell dysfunction, *Am. J. Physiol. Cell Physiol.* 280 (4) (2001) C719–C741.
- [67] M. Simionescu, Implications of early structural-functional changes in the endothelium for vascular disease, *Arterioscler. Thromb. Vasc. Biol.* 27 (2) (2007) 266–274.
- [68] D. Bernhard, A. Csordas, B. Henderson, A. Rossmann, M. Kind, G. Wick, Cigarette smoke metal-catalyzed protein oxidation leads to vascular endothelial cell contraction by depolymerization of microtubules, *FASEB J.* 19 (9) (2005) 1096–1107.
- [69] W. Seeger, T. Hansen, R. Rossig, T. Schmehl, H. Schutte, H.J. Kramer, D. Walmrath, N. Weissmann, F. Grimminger, N. Suttrop, Hydrogen peroxide-induced increase in lung endothelial and epithelial permeability—effect of adenylate cyclase stimulation and phosphodiesterase inhibition, *Microvasc. Res.* 50 (1) (1995) 1–17.